IOPscience iopscience.iop.org

Home Search Collections Journals About Contact us My IOPscience

Air-gun signature modelling considering the influence of mechanical structure factors

This content has been downloaded from IOPscience. Please scroll down to see the full text.

2014 J. Geophys. Eng. 11 025005

(http://iopscience.iop.org/1742-2140/11/2/025005)

View the table of contents for this issue, or go to the journal homepage for more

Download details:

IP Address: 171.66.208.130
This content was downloaded on 03/04/2015 at 17:23

Please note that terms and conditions apply.

IOP Publishing Journal of Geophysics and Engineering
J. Geophys. Eng. **11** (2014) 025005 (8pp) doi:10.1088/1742-2132/11/2/025005

Air-gun signature modelling considering the influence of mechanical structure factors

Guofa Li[1], **Zhao Liu**[1], **Jianhua Wang**[2] **and Mingqiang Cao**[3]

[1] Key Laboratory of Geophysical Exploration of China National Petroleum Corporation, China University of Petroleum, Beijing 102249, People's Republic of China
[2] CNOOC Research Institute, Beijing 100027, People's Republic of China
[3] BGP Offshore, PetroChina, Tianjin 300280, People's Republic of China

E-mail: liuzhaotony@163.com

Received 6 May 2013, revised 16 January 2014
Accepted for publication 21 January 2014
Published 4 April 2014

Abstract

In marine seismic prospecting, as the air-gun array is usually composed of different types of air-guns, the signature modelling of different air-guns is particularly important to the array design. Different types of air-guns have different mechanical structures, which directly or indirectly affect the signatures. In order to simulate the influence of the mechanical structure, five parameters—the throttling constant, throttling power law exponent, mass release efficiency, fluid viscosity and heat transfer coefficient—are used in signature modelling. Through minimizing the energy relative error between the simulated and the measured signatures by the simulated annealing method, the five optimal parameters can be estimated. The method is tested in a field experiment, and the consistency between the simulated and the measured signatures is improved with the optimal parameters.

Keywords: air-gun, signature, mechanical structure, optimization

(Some figures may appear in colour only in the online journal)

1. Introduction

After an air-gun is fired, high-pressure air is released into the surrounding infinite water medium and an air bubble is generated. The dynamic process of the air-gun bubble and the signature modelling have been discussed in many references. Keller and Kolodner (1956) took the high-pressure air to be a freely oscillating bubble of spherical shape and proposed the 'free oscillation bubble theory'. Based on this theory, Ziolkowski (1970), Schulze-Gattermann (1972) and Safer (1976) successively formulated their physical models used for simulating air-gun signatures. However, there are obvious differences between the measured and the simulated signatures based on the above models. On one hand, their models have not taken the port throttling effect into consideration, which makes the primary pulses of their signatures too large. On the other hand, these models only account for the attenuation of the bubble pluses via acoustic radiation, without considering the impacts of the fluid viscosity and the heat transfer between the bubble and fluid, which makes the decay of the bubble pulses too slow. Ziolkowski (1982) proposed a mechanism for the heat transfer across the bubble wall via the evaporation and condensation of water vapour. Laws *et al* (1990) analysed the mechanism of gun port throttling and concluded that the high-pressure air in the gun chamber is not released into the bubble instantaneously, which affects the air-gun signature. Langhammer (1993) quantified the effects of fluid viscosity upon the signature through an experimental study.

Considering the impacts of the port throttling effect, fluid viscosity and heat transfer on simulating air-gun signatures, Li *et al* (2010) improved Ziolkowski's model and finally formulated a more-accurate signature model. Yet, there are not systematic discussions on the signature simulation of a given type of air-gun. MacGillivray (2000) improved the signatures of different air-guns by optimizing the four parameters: the heat transfer coefficient, throttling constant, throttling power law exponent and mass release efficiency.

For different air-guns, their mechanical structures are different, which directly or indirectly affects the air-gun signature. Five parameters are introduced to account for the mechanical effects, which can be classified into two categories. One directly relates to the air-gun mechanical

 © 2014 Sinopec Geophysical Research Institute Printed in the UK

structure, including the throttling constant, throttling power law exponent and mass release efficiency; the other one indirectly relates to the mechanical structure, including the fluid viscosity and heat transfer coefficient. The five optimal parameters for a given air-gun can be estimated by minimizing the energy relative error between the simulated and the measured signatures. The optimization method is tested with synthetic and real signatures, and the consistency between the simulated and the measured signatures is improved with the five optimal parameters.

2. Air-gun signature modelling

After an air-gun is fired in an infinite compressible liquid, a spherical bubble forms rapidly and then oscillates harmonically. The pressure wave signature $P(r,t)$ in the liquid can be calculated by

$$P(r,t) = \rho\left[-\frac{\partial\varphi}{\partial t} - \frac{1}{2}\left(\frac{\partial\varphi}{\partial r}\right)^2\right], \tag{1}$$

where ρ is the liquid density, r is the distance between the air-gun source and hydrophone, φ is a scalar function referred to as the velocity potential, the gradient of which is the flow velocity of the fluid.

Keller and Kolodner (1956) proposed that φ satisfies the wave equation

$$\nabla^2\varphi - \frac{1}{c^2}\varphi_{tt} = 0, \tag{2}$$

where c is the sound velocity in the liquid. $\frac{\partial\varphi}{\partial t}$ and $\frac{\partial\varphi}{\partial r}$ can be expressed as

$$\frac{\partial\varphi}{\partial t} = -\frac{f'(a)}{r}, \tag{3}$$

$$\frac{\partial\varphi}{\partial r} = \frac{f'(a)}{cr} + \frac{f(a)}{r^2}, \tag{4}$$

where $f(a) = R^2(a)\dot{R}(a)$, $a = t - \frac{r}{c}$, R is the bubble radius and $\dot{R}$ is the bubble wall velocity. Thus, the pressure $P(r,t)$ is a function of R.

Herring (1941) expressed the bubble motion equation as

$$R\ddot{R}\left(1 - \frac{2\dot{R}}{c}\right) + \frac{3}{2}\dot{R}^2\left(1 - \frac{4\dot{R}}{3c}\right) + \frac{1}{\rho}\left(p_\infty - p - \frac{R}{c}\cdot\frac{\mathrm{d}p}{\mathrm{d}t}\right) = 0, \tag{5}$$

where $\ddot{R}$ is the acceleration of the bubble wall, p is the pressure on the bubble wall and p_∞ is the hydrostatic pressure. Equation (5) is a second-order nonlinear ordinary differential equation, which can be solved using an iteration method.

Prosperetti (1984) suggested that the relation between R and p can be expressed as

$$p = \frac{mR_GT}{V} + p_v - \frac{2\sigma}{R} - \frac{4\mu\dot{R}}{R}, \tag{6}$$

where m is the mass of the air in the bubble, R_G is the general gas constant, T is the temperature in the bubble, V is the volume of the air in the bubble, p_v is the constant vapour pressure, σ is the surface tension coefficient and μ is the fluid viscosity.

Due to the port throttling effect of the air-gun, the high-pressure air is not instantaneously released from the gun chamber into the bubble. As the bubble is an open thermodynamic system, the heat of the air in the bubble will spread to the surrounding fluid through the bubble wall during oscillation. Li *et al* (2010) showed that the mass injection rate $\mathrm{d}m/\mathrm{d}t$, the temperature variation $\mathrm{d}T/\mathrm{d}t$, the heat transfer rate $\mathrm{d}Q/\mathrm{d}t$ and the volume variation of the bubble $\mathrm{d}V/\mathrm{d}t$ can be expressed as

$$\frac{\mathrm{d}m}{\mathrm{d}t} = \tau_0(V_g)^\beta\sqrt{\frac{(p_g - p)m_g}{V_g}}, \tag{7}$$

$$\frac{\mathrm{d}T}{\mathrm{d}t} = \frac{R_GT\frac{\mathrm{d}m}{\mathrm{d}t} - \frac{\mathrm{d}Q}{\mathrm{d}t} - p\frac{\mathrm{d}V}{\mathrm{d}t}}{mc_v}, \tag{8}$$

$$\frac{\mathrm{d}Q}{\mathrm{d}t} = 4\pi R^2k(T - T_w), \tag{9}$$

$$\frac{\mathrm{dV}}{\mathrm{dt}} = 4\pi R^2\dot{R}, \tag{10}$$

where m_g is the mass of the air inside the gun chamber, V_g is the volume of the gun chamber, p_g is the pressure of the gun, τ_0 is the throttling constant, β is the throttling power law exponent, R_G is the general gas constant, c_v is the heat capacity of the air at constant volume, k is the heat transfer coefficient, T is the temperature in the bubble and T_w is the temperature of the surrounding fluid.

The signature $P(r,t)$ can be obtained in this way. At first, R, $\dot{R}$ and $\ddot{R}$ can be solved by equations (6) and (5). Then, $\frac{\partial\varphi}{\partial t}$ and $\frac{\partial\varphi}{\partial r}$ can be calculated by equations (3) and (4). Finally, $\frac{\partial\varphi}{\partial t}$ and $\frac{\partial\varphi}{\partial r}$ can be substituted into equation (1) to get signature $P(r,t)$.

It should be noted that, after the air-gun is fired, the air in the gun chamber is not completely released. Some air still remains in the gun chamber after the gun port closes. In the model, parameter η is used to denote the mass release efficiency

$$\eta = \frac{m_\infty}{m_g}, \tag{11}$$

where m_∞ is the mass of the total air in the bubble after the air-gun is fired, and m_g is the mass of the total air in the gun chamber before the air-gun is fired.

During the oscillation, the bubble moves up vertically with a velocity v_{up},

$$v_{\mathrm{up}} = \frac{2g}{R^3}\int_0^t R^3\,\mathrm{d}t, \tag{12}$$

where g is the acceleration due to gravity. However, in our research the vertical movement of the bubble is ignored for the reason that the bubble moves upward less than 1 m during the approximate 200 ms period of interest and that the vertical movement has hardly any influence on the signature within the period of interest. As is shown in figure 1, the two signatures with and without considering the vertical movement are almost overlapped.

From the discussion above, there are many factors affecting the air-gun signature. However, we focus on the factors associated with the mechanical structure of the air-gun.

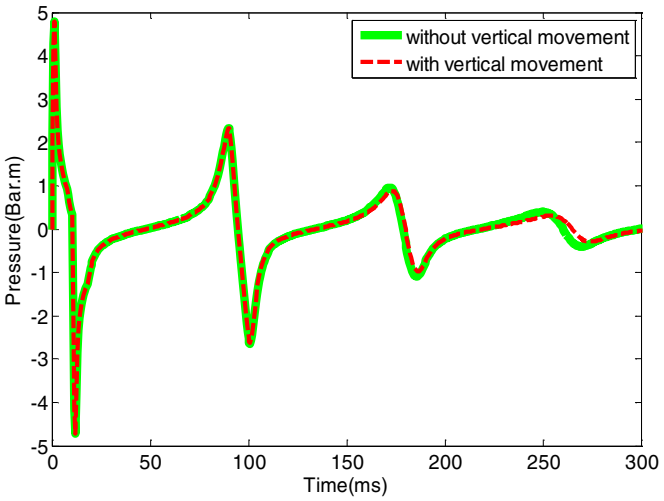


Figure 1. The air-gun signatures simulated with and without considering the vertical movement of the bubble.

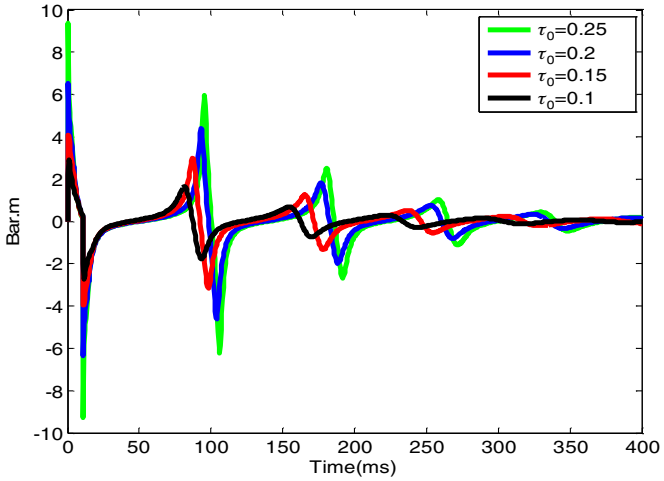


Figure 2. The air-gun signatures for $\tau_0 = 0.1$, $\tau_0 = 0.15$, $\tau_0 = 0.2$ and $\tau_0 = 0.25$. The firing pressure is 2000 psi, the gun volume is 100 cu in, the gun depth is 8 m, $\beta = 0.52$, $\eta = 0.8317$, $\mu = 100$ Pa s and $k = 10000$ W m^{-2} K^{-1}.

3. Effects of the air-gun mechanical structure

For a real air-gun, the area of the gun port should not be neglected, which results in a blocking effect on the high-pressure air released from the gun chamber. That is to say, the high-pressure air is released into the bubble in a very short time (about 2 ms) rather than instantaneously. So the pressure in the bubble is lower than in the gun chamber. This blocking effect is called the port throttling effect, and it is represented by the throttling constant τ_0 and the throttling power law exponent β in the air-gun model.

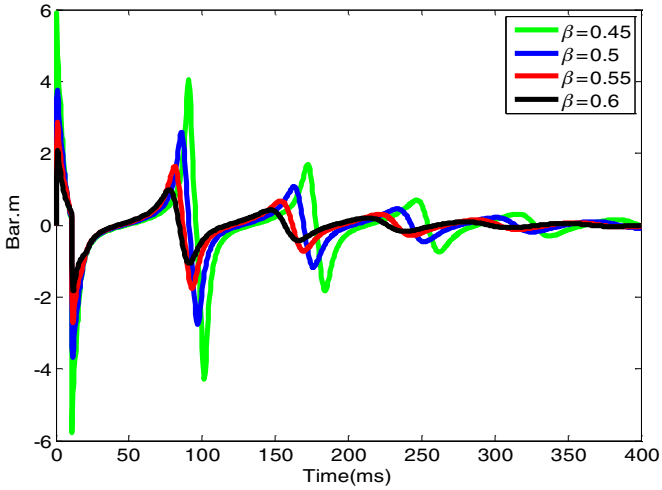


Figure 4. The air-gun signatures for $\beta = 0.45$, $\beta = 0.5$, $\beta = 0.55$ and $\beta = 0.6$. The firing pressure is 2000 psi, the gun volume is 100 cu in, the gun depth is 8 m, $\tau_0 = 0.12$, $\eta = 0.8317$, $\mu = 100$ Pa s and $k = 10000$ W m^{-2} K^{-1}.

τ_0 and β control the mass injection rate dm/dt during the high-pressure air release. The greater the port throttling effect, the smaller the mass injection rate. Different air-guns have different port throttling effects. In order to illustrate the influence on the air-gun signature imposed by the port throttling effect, different values of τ_0 and β are used to simulate signatures. From figures 2 and 3, it is evident that the primary pulse (the first positive peak of the air-gun signature), the bubble pulse (mainly the second positive peak) and the bubble period (the time interval between the first and second positive peaks) increase as τ_0 increases. Figures 4 and 5 show that the primary pulse, bubble pulse and bubble period decrease as β increases.

After the gun port is closed, there is still some air remaining in the gun chamber. The mass release efficiency η depends on the air-gun mechanical structure. In figures 6

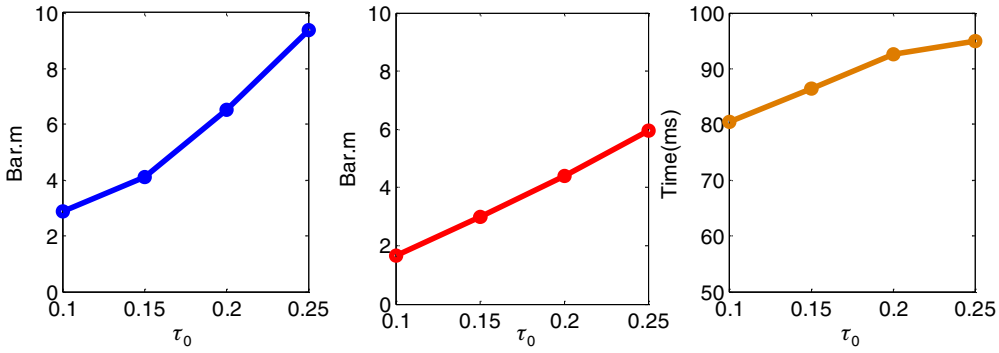


Figure 3. The variation of primary pulse (left), bubble pulse (middle) and bubble period (right) with τ_0.

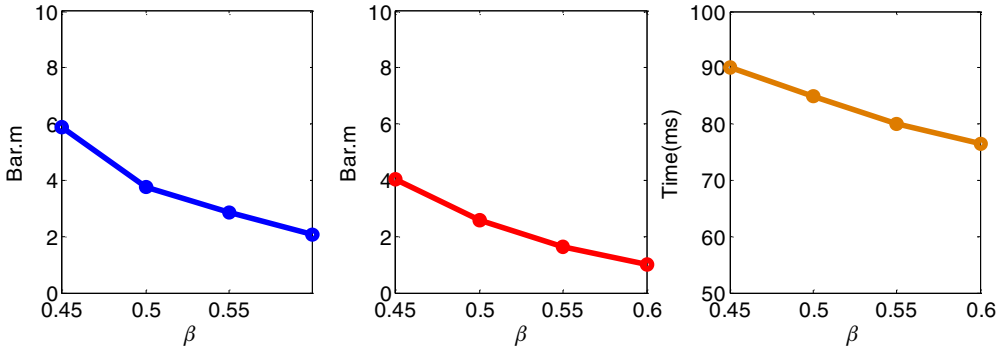


Figure 5. The variation of the primary pulse (left), bubble pulse (middle) and bubble period (right) with β.

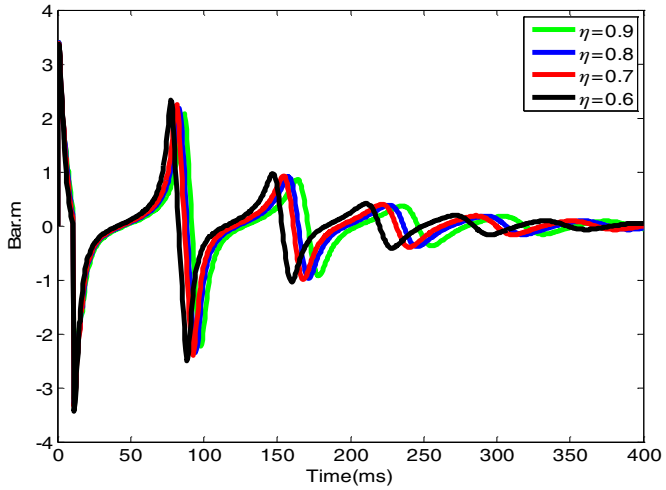


Figure 6. The air-gun signatures for $\eta = 0.6$, $\eta = 0.7$, $\eta = 0.8$ and $\eta = 0.9$. The firing pressure is 2000 psi, the gun volume is 100 cu in, the gun depth is 8 m, $\tau_0 = 0.12$, $\beta = 0.52$, $\mu = 100$ Pa s and $k = 10\,000$ W m^{-2} K^{-1}.

and 7, signatures are simulated using different η to illustrate the effects. It can be seen that the primary pulse and bubble pulse change little while the bubble period becomes longer when η becomes larger.

After the high-pressure air is released, the velocity of the fluid motion increases and the flow becomes turbulent. Laws *et al* (1990) considered that the turbulence is always present in the fluid near the bubble wall. The turbulent eddies greatly increase the viscosity of the surrounding water and the heat transfer across the bubble wall, which significantly affects the damping of the bubble. The generation of turbulence is related to the air-gun mechanical structure, thus the fluid viscosity μ and the heat transfer coefficient k can be considered as indirect mechanical factors to the air-gun signature.

On one hand, the eddies increase the viscosity of the water to a large 'effective' viscosity μ_{eff},

$$\mu_{\text{eff}} = \mu_0 \left(1 + KR_e\right), \tag{13}$$

where μ_0 is the classical viscosity, K is a constant (about 0.02), and R_e is the Reynolds number. On the other hand, the eddies also greatly increase the rate of heat transfer. This is because, instead of being transported at the molecular level, the heat is conducted by the bulk movement of water resulting from the eddies. So k is also an 'effective' heat transfer coefficient. The viscosity and the heat transfer coefficient in the air-gun signature model are greatly larger than the classical values. Figures 8 and 9 show that the viscosity μ mainly affects the bubble pulse, and the larger the μ, the lower the bubble pulse. From figures 10 and 11, it is can be seen that the larger the k, the lower the bubble pulse and the shorter the bubble period.

From the analysis above, the five parameters associated with the air-gun mechanical structure can be classified into two categories. One directly relates to the mechanical structure including the throttling constant τ_0, throttling power law exponent β and mass release efficiency η; the other one indirectly relates to the mechanical structure including the fluid viscosity μ and heat transfer coefficient k. The five parameters affect the primary pulse, bubble pulse and bubble period of the air-gun signature to different degrees.

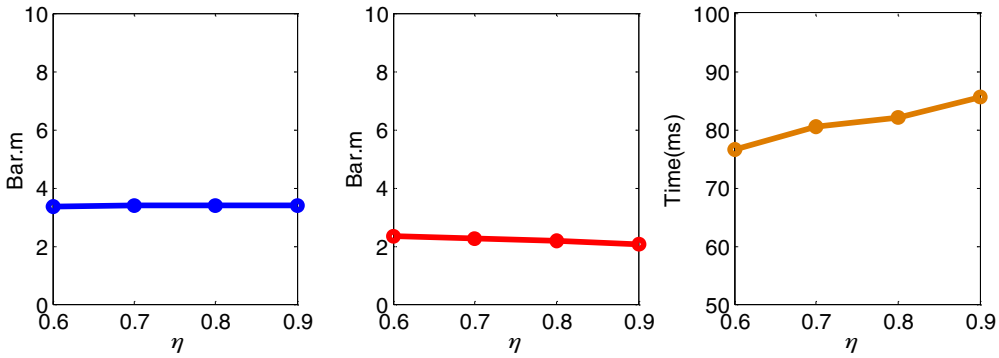


Figure 7. The variation of the primary pulse (left), bubble pulse (middle) and bubble period (right) with η.

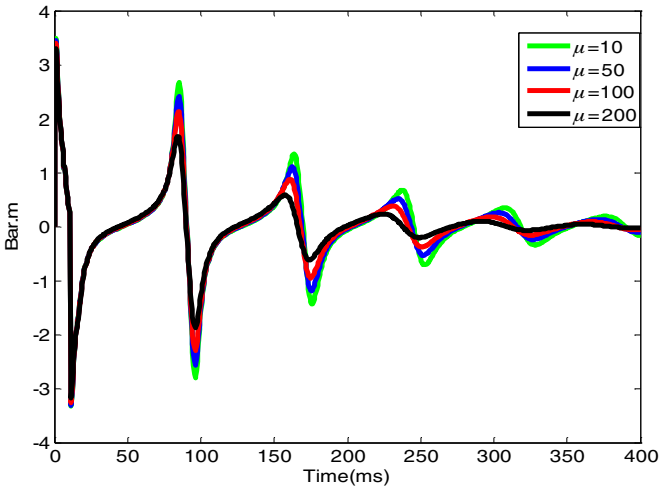


Figure 8. The air-gun signatures for $\mu = 10$ Pa s, $\mu = 50$ Pa s, $\mu = 100$ Pa s and $\mu = 200$ Pa s. The firing pressure is 2000 psi, the gun volume is 100 cu in, the gun depth is 8 m, $\tau_0 = 0.12$, $\beta = 0.52$, $\eta = 0.8317$ and $k = 10\,000$ W m^{-2} K^{-1}.

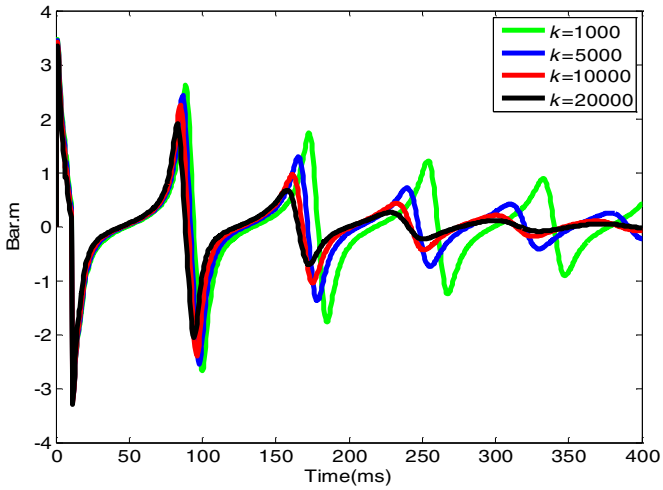


Figure 10. The air-gun signatures for $k = 1000$ W m^{-2} K^{-1}, $k = 5000$ W m^{-2} K^{-1}, $k = 10000$ W m^{-2} K^{-1} and $k = 20\,000$ W m^{-2} K^{-1}. The firing pressure is 2000 psi, the gun volume is 100 cu in, the gun depth is 8 m, $\tau_0 = 0.12$, $\beta = 0.52$, $\eta = 0.8317$ and $\mu = 100$ Pa s.

4. Estimation of mechanical parameters

The five parameters associated with the air-gun mechanical structure, throttling constant τ_0, throttling power law exponent β, mass release efficiency η, fluid viscosity μ and heat transfer coefficient k, can be estimated from a recorded pressure signal by minimizing the energy relative error between the simulated and the measured signature. The objective function can be defined as

$$F(\tau_0, \beta, \eta, \mu, k) = \frac{\sum_{i=1}^{N} (S_m(i\Delta t) - S_d(i\Delta t))^2}{\sum_{i=1}^{N} S_d^2(i\Delta t)}, \quad (14)$$

where S_m is the simulated signature, S_d is the measured signature, N is the sample number and Δt is the sample interval.

To avoid a local minimum trap, the Metropolis simulated annealing method is chosen to solve the optimization problem of equation (14) with the following steps:

(1) Set the initial values of the five parameters $(\tau_0, \beta, \eta, \mu, k)$ within the searching ranges.
(2) Set the initial temperature to T_0 and use the hyperbolic decline type as the cooling method so $T_i = T_0 (0.99)^i$, where i is the cooling number.
(3) For each temperature T_i, set the iteration number as L. In each iteration:
   (a) according to a uniform probability distribution, generate new parameters $(\tau_0', \beta', \eta', \mu', k')$ within the ranges randomly;
   (b) calculate the increment of the objective function
   $$\Delta F = F(\tau_0', \beta', \eta', \mu', k') - F(\tau_0, \beta, \eta, \mu, k);$$
   (c) use the Metropolis criterion to determine whether to accept the parameters $(\tau_0', \beta', \eta', \mu', k')$. If $\Delta F < 0$, accept the parameters; else compare $P = e^{\frac{-\Delta F}{T_i}}$ with a random number D ranging from 0 to 1. If $P > D$, accept the parameters; else reject the parameters;
   (d) return to step (a) to the next iteration.
(4) If $T_i > 1$, return to step (3); else stop iteration and output the current parameters as the optimal parameters.

5. Parameters estimation test based on the theoretical model

A model experiment is designed to validate the estimation of the mechanical parameters. The pressure of the air-gun is 2000 psi and the volume of air is 100 cu in. The air-gun is fired

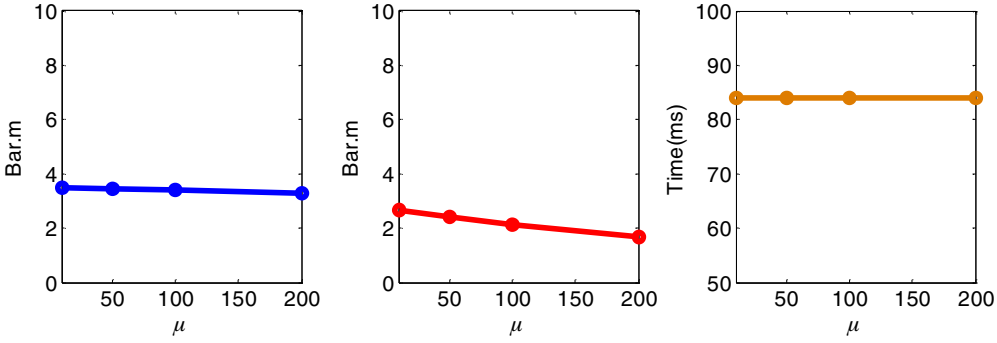


Figure 9. The variation of the primary pulse (left), bubble pulse (middle) and bubble period (right) with μ.

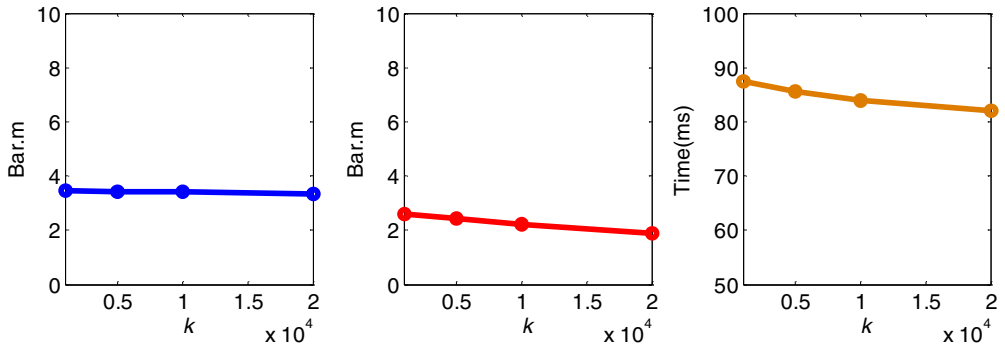


Figure 11. The variation of the primary pulse (left), bubble pulse (middle) and bubble period (right) with k.

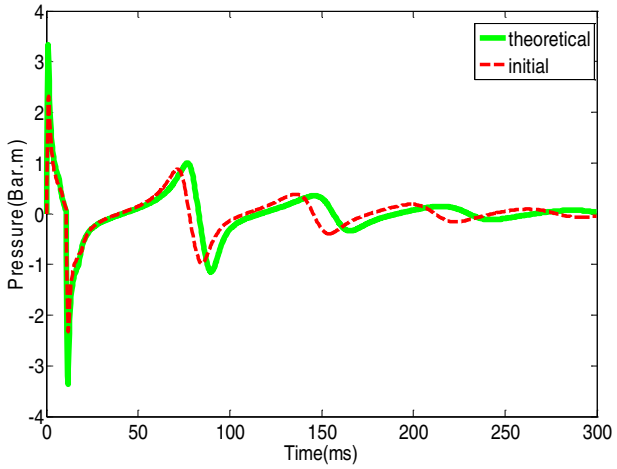


Figure 12. The comparison between the initial signature (red dashed curve) and the theoretical signature (green solid curve).

at 8 m below sea level. The temperature of the sea is about 20 °C and the sound velocity in the liquid is about 1500 ms^{-1}. The five parameters associated with the mechanical structure of the air-gun are given as

$$\tau_0 = 0.12$$
$$\beta = 0.52$$
$$\eta = 0.8317$$
$$\mu = 100.0\ \mathrm{Pa\,s}$$
$$k = 22\,230.0\ \mathrm{W\,m^{-2}\,K^{-1}}.$$

The theoretical signature corresponding to the above parameters is simulated and shown in the green solid curve in figure 12.

The initial values of the five parameters are set as

$$\tau_0 = 0.15$$
$$\beta = 0.62$$
$$\eta = 0.7$$
$$\mu = 80.0\ \mathrm{Pa\,s}$$
$$k = 18\,230.0\ \mathrm{W\,m^{-2}\,K^{-1}}.$$

The signature simulated with the initial mechanical parameters is shown in the red dashed curve in figure 12. The initial signature is obviously different from the theoretical signature in primary amplitude, bubble pulse and attenuation velocity, with the energy relative error 0.1831.

The searching range for each parameter should be given before iteration. The minimum values of τ_0 and β are usually set as zero, which means that the port throttling effect is neglected, and the maximum values of τ_0 and β are usually set as 1.0, since a larger value than 1.0 will generate a simulated signature which is far from the reasonable signature. The range of parameter η is set from 0.0 to 1.0, meaning a complete release and no release, respectively. The maximum values of μ and k are also experimental parameters: when $\mu > 500$ Pa s or $k > 50\,000\ \mathrm{W\,m^{-2}\,K^{-1}}$, the primary pulse is affected seriously by the turbulent eddies, which has never been observed in practice. Therefore, the searching ranges of the five parameters are set as

$$\tau_0 \in (0, 1.0)$$
$$\beta \in (0, 1.0)$$
$$\eta \in (0, 1.0)$$
$$\mu \in (0, 500]\ \mathrm{Pa\,s}$$
$$k \in (0, 50\,000]\ \mathrm{W\,m^{-2}\,K^{-1}}.$$

After 43 700 iterations, the optimal mechanical parameters are obtained as

$$\tau_0 = 0.12$$
$$\beta = 0.52$$
$$\eta = 0.8400$$
$$\mu = 114.0\ \mathrm{Pa\,s}$$
$$k = 22\,700.0\ \mathrm{W\,m^{-2}\,K^{-1}}.$$

The signature with optimal parameters and the theoretical signature are visually indistinguishable and the energy relative error is reduced to 0.000 57 from the initial 0.1831.

6. Parameters' estimation test based on the field measured signature

To test and estimate the influencing factors of the air-gun signature, BGP Offshore conducted air-gun signal acquisition tests in the Red Sea near Farasan Island in 2012. This air-gun is a G gun. The firing pressure is 2000 psi and the volume of the air is 40 cu in. The depths of the G gun and the hydrophone are 7 m and 300 m, respectively. The temperature is about 20 °C and the sound velocity in the liquid is about 1500 ms^{-1}. The measured signature is shown in green solid curve in figure 13.

The initial values of the mechanical parameters are set as

$$\tau_0 = 0.15$$
$$\beta = 0.7$$
$$\eta = 0.7$$
$$\mu = 50.0\ \mathrm{Pa\,s}$$
$$k = 500.0\ \mathrm{W\,m^{-2}\,K^{-1}}.$$

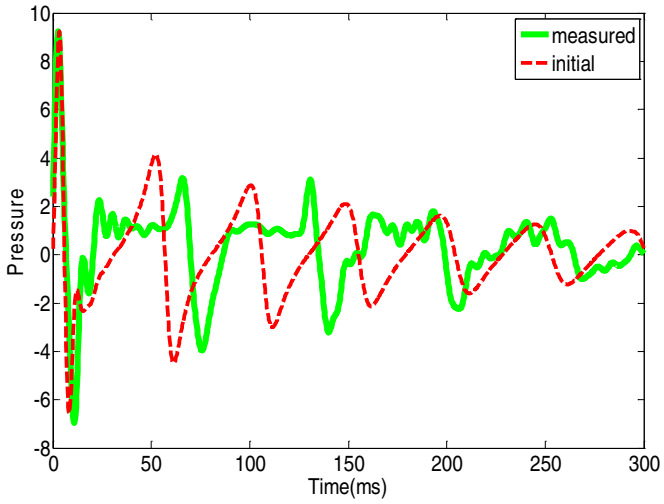


Figure 13. The comparison between the initial signature (red dashed curve) and the measured signature (green solid curve).

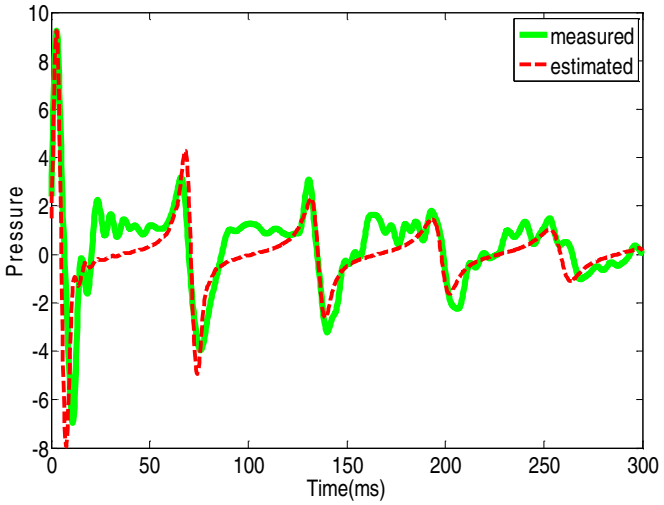


Figure 14. The comparison between the estimated signature (red dashed curve) and the measured signature (green solid curve).

The corresponding initial signature is shown in the red dashed curve in figure 13. The initial signature is far from the measured signature with an energy relative error of 0.9013.

After 87 400 iterations, the final estimated parameters are obtained as

$$\tau_0 = 0.30$$
$$\beta = 0.55$$
$$\eta = 0.9387$$
$$\mu = 89.0\ \text{Pa s}$$
$$k = 942.0\ \text{W m}^{-2}\ \text{K}^{-1}.$$

The corresponding estimated signature is shown in the red dashed curve in figure 14, with the measured signature displayed in the green solid curve. Compared to the initial signature, the consistency between the estimated and the measured signature is improved significantly, with the energy relative error reduced to 0.3342.

From figure 14, it is noticeable that there are at least two differences between the estimated and the measured signature. One difference is the series of irregular ripples of high frequency in the measured signature which is not well simulated; another one is that the transition zone between the primary pulse and the bubble pulse in the measured signature is flatter than in the estimated signature. The former difference may be attributed to marine noise or possibly something related to the force reaction in the gun, but the latter difference cannot be well explained within our scope of knowledge. The theory of the air-gun signature is expected to be developed to more-accurately represent what occurs in a real situation. The optimization method should also be improved and the determination of certainty in the estimation of the five mechanical parameters should be further studied in future work.

7. Conclusions

Two categories of parameters associated with a mechanical structure are introduced in air-gun signature modelling. One directly relates to the air-gun mechanical structure, including throttling constant, throttling power law exponent and mass release efficiency; the other one indirectly relates to the air-gun mechanical structure, including fluid viscosity and heat transfer coefficient. Through minimizing the energy relative error between the simulated and the measured signatures by simulated annealing optimization, the five mechanical parameters can be optimally estimated. With the optimal mechanical parameters, the air-gun signature, considering the influence of mechanical structure factors, is simulated. Since the air-gun array is usually composed of air-guns of different mechanical structure, the estimation of the mechanical parameters will play a useful role in air-gun array design.

Acknowledgments

This research is financially supported by the National Natural Science Foundation of China (grant no 41174117) and Major National Science and Technology Projects (2011ZX05031–001). BGP Offshore provided the measured signature.

References

Herring C 1941 Theory of the pulsations of the gas bubble produced by an underwater explosion *OSRD Report* 236

Keller J B and Kolodner I I 1956 Damping of underwater explosion bubble oscillations *J. Appl. Phys.* **27** 1152–61

Laws R M, Hatton L and Haartsen M 1990 Computer modeling of clustered air guns *First Break* **8** 331–8

Langhammer M L 1993 Experimental study of viscosity effects on air gun signatures *Geophysics* **58** 1801–08

Li G F, Cao M Q, Chen H L and Ni C Z 2010 Modeling air gun signatures in marine seismic exploration considering multiple physical factors *Appl. Geophys.* **7** 158–65

MacGillivray A O 2000 An acoustic modeling study of seismic air gun noise in Queen Charlotte Basin *MSc Thesis* University of Victoria, Canada

Prosperetti A 1984 Bubble phenomena in sound fields: part one *Ultrasonics* **22** 69–77
Schulze-Gattermann R 1972 Physical aspects of the 'airpulse' as a seismic energy source *Geophys. Prospect.* **20** 155–92
Safer M H 1976 Efficient design of air-gun arrays *Geophys. Prospect.* **24** 773–87
Ziolkowski A 1970 A method for calculating the output pressure waveform from an air-gun *Geophys. J. R. astron. Soc.* **21** 137–61
Ziolkowski A 1982 An air gun model which includes heat transfer and bubble interaction *SEG Expanded Abstract* pp 187–9